Journal of Alloys and Compounds 504S (2010) S74–S77

Contents lists available at ScienceDirect

Journal of Alloys and Compounds

journal homepage: www.elsevier.com/locate/jallcom

The effect of microalloying on mechanical properties in CuZrAl bulk metallic glass

J. Pan [a], K.C. Chan [b], Q. Chen [a], N. Li [a], S.F. Guo [a], L. Liu [a,*]

[a] State Key Laboratory of Material Processing and Die & Mould Technology, Huazhong University of Science and Technology, 430074 Wuhan, China
[b] Department of Industrial System and Engineering, The Hong Kong Polytechnic University, Hong Kong, China

ARTICLE INFO

Article history:
Received 6 July 2009
Received in revised form 9 January 2010
Accepted 10 February 2010
Available online 18 February 2010

Keywords:
Bulk metallic glass
Microalloying
Plasticity
Phase separation

ABSTRACT

The effect of the minor addition of elements Ta and Fe on the mechanical properties of the CuZrAl BMG was investigated by compression tests. It was found that the addition improves significantly the plasticity at room temperature. The compressive plastic strain enhanced from 0.59% for $Cu_{46}Zr_{47}Al_7$ BMG to 2.62% and 4.81% for $Cu_{46}Zr_{45}Al_7Ta_2$ and $Cu_{44}Zr_{47}Al_7Fe_2$ BMG, respectively. The microstructure of $Cu_{44}Zr_{47}Al_7Fe_2$ BMG was further investigated by TEM, which reveals the occurrence of phase separation with the formation of a Cu-rich phase and a Fe-rich phase due to the minor addition of Fe. The formation of inhomogeneous structure in amorphous phase, which results in the activation of multi shear bands, can account for the improvement of the plasticity of the base BMG. The present results provide a promising approach to enhance the plasticity of BMGs through compositional and structural design by microalloying.

1. Introduction

Compared to traditional crystalline metallic materials, bulk metallic glasses (BMGs) with atomically amorphous structure exhibit unique mechanical properties, including high fracture strength and hardness, excellent corrosion resistance and fatigue durability [1–3], but with only limited room temperature plasticity before fracture [4,5]. Many approaches have been investigated to improve the plasticity of BMGs, such as to introduce micrometer-size ductile crystalline phase [6], to form nano-size structural heterogeneity [7,8] and to enhance the Poisson's ratio of the alloy [9,10].

The minor addition, has been widely used to control the manufacture, structure and properties of various crystalline materials, and is now applied to BMGs to improve their plasticity [11–15]. Xing [12] reported that the extended plasticity could be achieved in Zr-based BMGs containing minor refractory metals Ta, due to the formation of strong short-range ordering structure in amorphous phase. The similar result was also reported by Park [13] in $Cu_{47}Ti_{33}Zr_{11}Ni_8Si_1$ BMG. On the other hand, Chen [14] found that the $Cu_{45}Zr_{46}Al_7Ti_2$ BMG exhibits superior compressive plastic strain of 32.5%, and attributed the outstanding plasticity to the creation of a large amount of free volume in BMGs by the addition of a small amount of Ti. In this paper, based on the $Cu_{46}Zr_{47}Al_7$ amorphous system, we attempted to develop a new BMG with extended plasticity by addition of a trace amount of Ta and Fe, which have a positive heat of mixing with the main constituents in the based alloy.

2. Experimental

Alloy ingots with nominal composition of $Cu_{46}Zr_{47}Al_7$, $Cu_{46}Zr_{45}Al_7Ta_2$ and $Cu_{44}Zr_{47}Al_7Fe_2$ were prepared from elemental metals (purity >99.5%) by arc-melting under a Ti gettered Ar atmosphere. From the master alloy, sample rods with diameter of 2 mm and length of 70 mm were produced by copper mould casting for each composition. The amorphous structure of the as-cast alloys prepared was examined by X-ray diffraction (XRD, Philips χ' Pert Pro) with Cu Kα radiation and differential scanning calorimetry (DSC, Perkin-Elmer DSC-7) at a heating rate of 20 K/min. The detailed microstructure of as-cast samples was further examined by a transmission electron microscopy (TEM, Joel-2010) with nanobeam EDX. The TEM foils were prepared following a series of thinning processes, namely mechanopolishing, dimpling and finally ion-milling.

The uniaxial compression test was performed with a Zwick/Roell 020 testing machine at a strain rate of $1 \times 10^{-4}\ s^{-1}$. At least five specimens were tested for each composition to get a statistical result. The compression specimens with a diameter of 2 mm and a length of 4 mm were cut from the cast rods, and the ends were polished carefully to ensure parallelism. The morphology of fractured and the lateral surfaces of samples after fracture were examined with a scanning electron microscope (SEM, FEI Quanta 200).

3. Results and discussion

Fig. 1(a) shows the XRD patterns of as-cast alloys with a diameter of 2 mm. No distinct crystalline peaks are detected in the

* Corresponding author at: Department of Materials Science and Engineering, Huazhong University of Science and Technology, Louyu Road 1037, 430074 Wuhan, Hubei, China. Tel.: +86 27 87556894; fax: +86 27 87554405.
E-mail address: lliu2000@mail.hust.edu (L. Liu).

0925-8388/$ – see front matter © 2010 Elsevier B.V. All rights reserved.
doi:10.1016/j.jallcom.2010.02.064

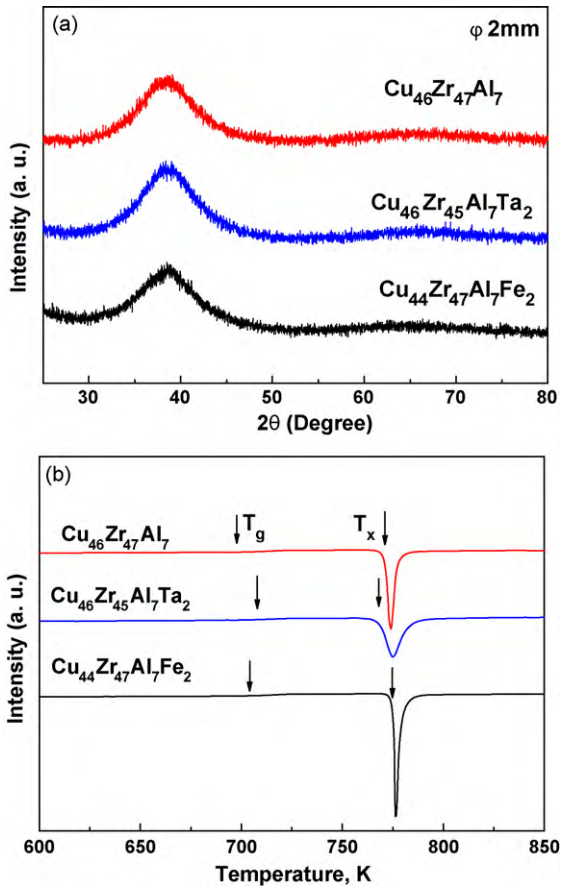

Fig. 1. XRD patterns (a) and DSC traces (b) of the as-cast alloys with 2 mm in diameter.

Table 1
The glass transition temperature T_g, the onset crystallization temperature T_x and the width of the supercooled liquid region ΔT_x together with the crystallization enthalpy ΔH for the various BMGs.

Samples	T_g (K)	T_x (K)	ΔT_x (K)	ΔH (J/g)
$Cu_{46}Zr_{47}Al_7$	697.7	771.2	73.5	−56.2
$Cu_{46}Zr_{45}Al_7Ta_2$	707.8	768.2	60.4	−57.1
$Cu_{44}Zr_{47}Al_7Fe_2$	704.1	774.7	70.6	−51.9

XRD spectra, indicating that all the alloys are basically amorphous. The DSC traces (Fig. 1(b)) of the as-cast alloys are quite similar with a distinct glass transition (T_g) and wide supercooled liquid region (ΔT_x) before crystallization. The various thermal parameters derived from DSC curves are listed in Table 1. It can be seen that the minor addition of the elements enhances the glass transition temperature, but decreases slightly the supercooled region.

Table 2
Mechanical properties of yield strength (σ_y), fracture strength (σ_f), elastic strain (ε_y), plastic strain (ε_p), and shear fracture angle (θ_f) of the various BMGs under uniaxial compression.

Samples	σ_y (MPa)	σ_f (MPa)	ε_y (%)	ε_p(%)	θ_f (°)
$Cu_{46}Zr_{47}Al_7$	1835	1922	1.63	0.59	39.5
$Cu_{46}Zr_{45}Al_7Ta_2$	1671	1906	1.55	2.62	41
$Cu_{44}Zr_{47}Al_7Fe_2$	1733	1956	2.02	4.81	41.5

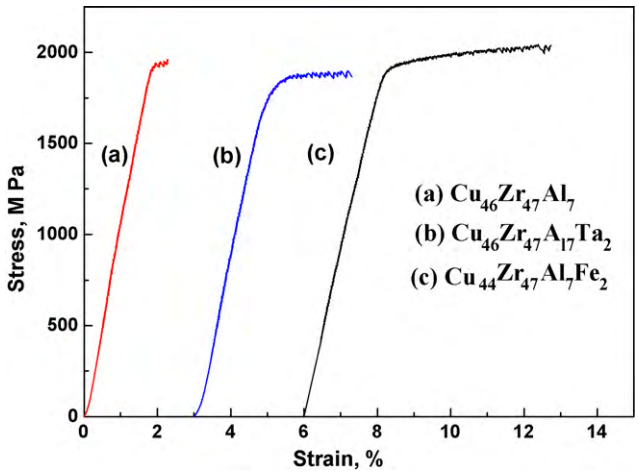

Fig. 2. Compressive stress–stain curves of the various BMGs at room temperature.

Fig. 2 shows the room temperature engineering stress–strain curves of various BMGs under uniaxial compression at a stain rate of $1 \times 10^{-4}\ s^{-1}$, from which the yield strength (σ_y), fracture strength (σ_f), elastic strain (ε_y), and plastic strain (ε_p) are obtained and summarized in Table 2. It can be seen that there is no much difference in the fracture strength with the addition of Ta and Fe as compared with the base alloy, but significant enhancement of plasticity could be achieved due to the addition. For instance, $Cu_{46}Zr_{47}Al_7$ BMG exhibits very limited plasticity of about 0.59% before failure, however, $Cu_{46}Zr_{45}Al_7Ta_2$ and $Cu_{44}Zr_{47}Al_7Fe_2$ BMGs show pronounced enhanced plastic strain of 2.61% and 4.81%, respectively.

All the BMGs failed along a main shear band with the shear fracture angle (θ_f) around 40° (see Table 2), which is smaller than 45°, indicating that the deformation mechanism of the BMGs in the present study follows the Mohr–Coulomb criterion. The shear bands on the lateral surface and fracture patterns of the failure samples are shown in Fig. 3. Only few shear bands was found in $Cu_{46}Zr_{47}Al_7$ BMG (Fig. 3(a)), while multiple shear bands could be observed in $Cu_{46}Zr_{45}Al_7Ta_2$ and $Cu_{44}Zr_{47}Al_7Fe_2$ BMGs (Fig. 3(c) and (e)). Since the plastic deformation achieved in bulk metallic glasses is confined almost entirely to the narrow regions in the shear bands, the high density and the extensive distribution of the shear bands should account for the enhanced plasticity. On the other hand, the fracture surface of $Cu_{46}Zr_{47}Al_7$ and $Cu_{46}Zr_{47}Al_7Ta_2$ BMG displays vein-like patterns, which is typical feature for amorphous alloys. But $Cu_{44}Zr_{47}Al_7Fe_2$ BMG exhibits an unique fracture morphology consisting of both vein-like and river-like patterns, which may result from the continuous change in the propagation direction of shear bands. Similar fracture morphology was also observed in some other BMGs with good room temperature plasticity [16].

To understand the effect of the minor additions on the improvement of the plasticity of the base BMG, the microstructure of $Cu_{46}Zr_{47}Al_7$ and $Cu_{44}Zr_{47}Al_7Fe_2$ BMGs was comparatively investigated by TEM. The TEM bright-field image of the as-cast $Cu_{46}Zr_{47}Al_7$ BMG, exhibits a uniform contrast with a diffused electron diffraction pattern (see Fig. 4(a)), indicating a homogeneous amorphous structure of the alloy. In contrast, the bright-field image of the $Cu_{44}Zr_{47}Al_7Fe_2$ BMG shows apparently the presence of two different phases with brighter and darker contrasts (Fig. 4(b)). The electron diffraction pattern does not show any diffraction spots, implying that the light and dark contrast phases are all amorphous. Nanobeam EDX analysis revealed that the dark phase is enriched with Fe, while the light matrix is enriched with Cu. The characteristic length scale

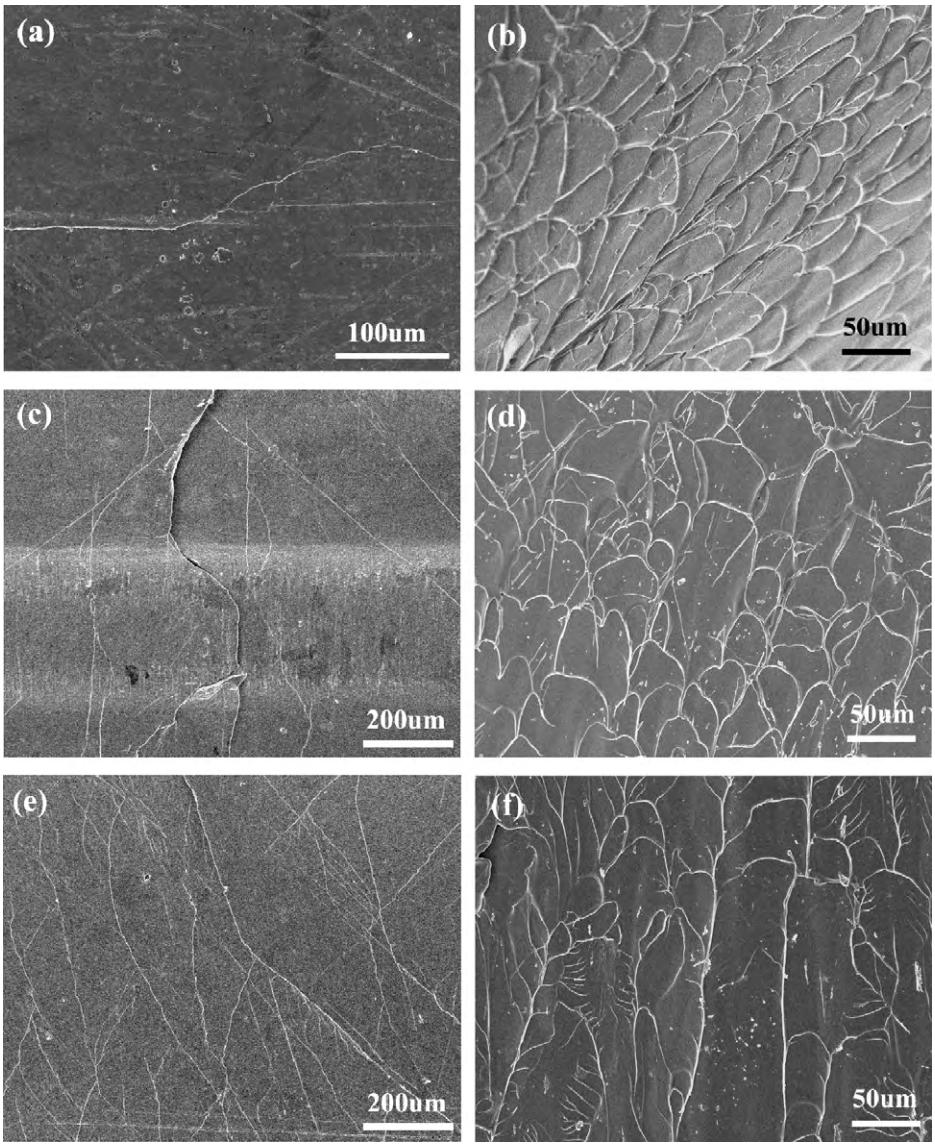

Fig. 3. SEM images of the outer appearance and fracture surface of $Cu_{46}Zr_{47}Al_7$ (a and b), $Cu_{46}Zr_{45}Al_7Ta_2$ (c and d) and $Cu_{44}Zr_{47}Al_7Fe_2$ (e and f) BMGs after compression to fracture.

for the dark phases is about 10–20 nm. This means that amorphous nano-scale phase separation occurred in $Cu_{44}Zr_{47}Al_7Fe_2$ system.

Microalloying has been proven to be an effective way to enhance the plasticity of BMGs, especially when the alloyed element that has a positive enthalpy of mixing with the main constituent in the base alloy, which may lead to phase separation in the as-cast state [17–21]. In the present system, the relationship of mixing heat among constituent elements is shown in Fig. 5. Ta has large negative heat of mixing with Al, while has positive heat of mixing with Zr and Cu (+3 kJ/mol for Ta–Zr and +2 KJ/mol for Ta–Cu, respectively). Therefore, partial replacement of Zr by Ta in CuZrAl system may result in the formation of an inhomogeneous structure, such as strong short-range or medium-range ordering clusters in the amorphous phase, which can improve the plasticity of the $Cu_{46}Zr_{45}Al_7Ta_2$ BMG [22]. The similar results had also been reported previously by Hufnagel [23,24]. On the other hand, Fe and Cu show a positive heat of mixing of +13 kJ/mol, which is much larger than Zr and Ta, while Fe has a large negative heat of mixing with the three remaining elements Cu, Zr and Al. In such a case, phase separation could most likely take place due to the energetically favorability, which is actually realized in this study. The $Cu_{44}Zr_{47}Al_7Fe_2$ BMG has two amorphous phases with different chemical compositions, thus should have a different modulus and critical shear stresses (CSSs) in the BMG. Upon deformation, when a shear band is initiated preferentially, its propagation might be hindered by other glass domains with higher CSS. Then, the propagation of the shear band would be retarded, resulting in initiation and multiplication of new shear bands, which finally causes the enhancement of plasticity [25]. It is generally considered that the addition of alloying element having small positive heat of mixing with constituent elements might provide atomic-scale local chemical inhomogeneity or fluctuation in local free volume distribution, while the addition of alloying element having large positive heat of mixing with one constituent element could lead to phase separation. Both approaches can affect the propagation of the shear bands and cause the enhancement of the plasticity of BMG.

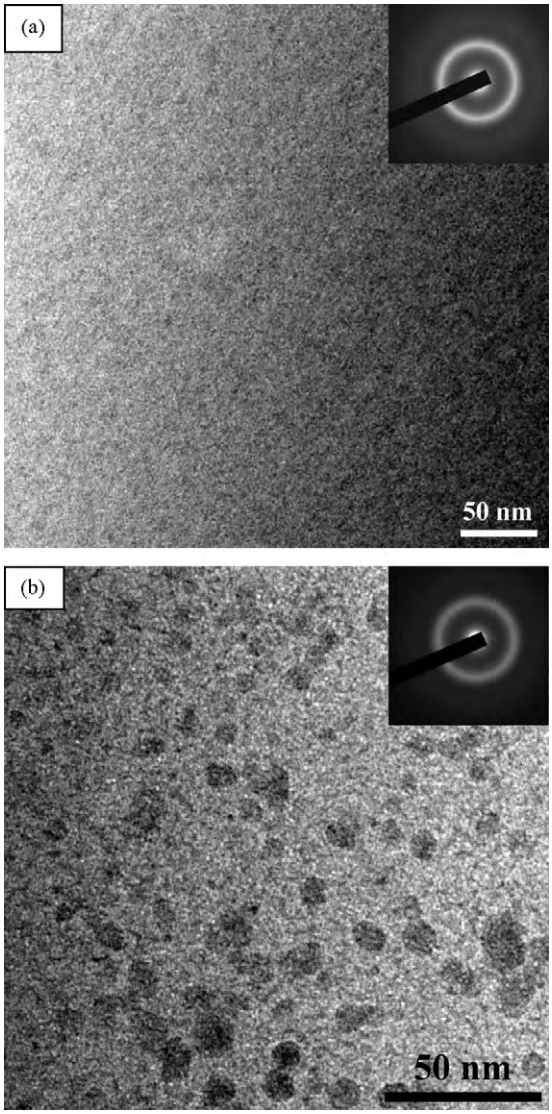

Fig. 4. TEM bright-field images with the inset of selected-area diffraction patterns for $Cu_{46}Zr_{47}Al_7$ (a) and $Cu_{44}Zr_{47}Al_7Fe_2$ (b) BMGs.

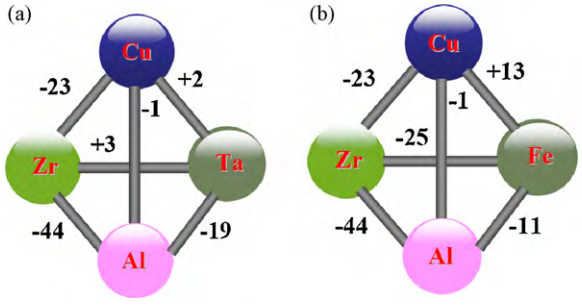

Fig. 5. Relationship of heat of mixing among constituent elements in CuZrAlM (M = Ta and Fe) alloy system.

4. Conclusions

The enhancement of plasticity of CuZrAl BMG was achieved by minor addition of Ta and Fe. The compressive plastic strain is enhanced from 0.59% for $Cu_{46}Zr_{47}Al_7$ BMG to 2.62% and 4.81% for $Cu_{46}Zr_{45}Al_7Ta_2$ and $Cu_{44}Zr_{47}Al_7Fe_2$ BMG, respectively. The generation of inhomogeneous structures either in the form of strong short/middle-range ordering or in the form of amorphous phase separation in amorphous phase due to the addition is responsible for the enhancement of the plasticity for $Cu_{46}Zr_{45}Al_7Ta_2$ and $Cu_{44}Zr_{47}Al_7Fe_2$ BMG. This present work provides a hint for the improvement of the mechanical properties of BMGs by microalloying, especially the large positive heating mixing with one element due to formation of nano-scale phase separation.

Acknowledgements

This work was financially supported by National Nature Science Foundation of China under grant No. 50871042 and 50828101. This work is also partially supported by the Research Grants Council of Hong Kong Special Administration Region (under the project code PolyU5111/08E). Authors are grateful to the Analytical and Testing Center, Huazhong University of Science & Technology for technical assistances.

References

[1] W.H. Wang, C. Dong, C.H. Shek, Mater. Sci. Eng. R 44 (2004) 45.
[2] A. Inoue, Acta Mater. 48 (2000) 279.
[3] W.L. Johnson, MRS Bull. 24 (1999) 42.
[4] Z.F. Zhang, G. He, J. Eckert, L. Schultz, Phys. Rev. Lett. 91 (2003) 045505.
[5] A. Inoue, B.L. Shen, H. Koshiba, H. Kato, A.R. Yavari, Nature Mater. 2 (2003) 661.
[6] Y. Zhang, A.L. Greer, Appl. Phys. Lett. 89 (2006) 071907.
[7] C.C. Hays, C.P. Kim, W.L. Johnson, Phys. Rev. Lett. 84 (2000) 2901.
[8] J. Das, M.B. Tang, K.B. Kim, R. Theissmann, F. Baier, W.H. Wang, J. Eckert, Phys. Rev. Lett. 94 (2005) 205501.
[9] K.B. Kim, J. Das, F. Baier, M.B. Tang, W.H. Wang, J. Eckert, Appl. Phys. Lett. 88 (2006) 051911.
[10] J. Schroers, W.L. Johnson, Phys. Rev. Lett. 93 (2004) 25506.
[11] W.H. Wang, Prog. Mater. Sci. 52 (2007) 540.
[12] L.Q. Xing, Y. Li, K.T. Ramesh, J. Li, T.C. Hufnagel, Phy. Rev. B 64 (2001) 180201.
[13] E.S. Park, D.H. Kim, T. Ohkubo, K. Hono, J. Non-Cryst. Solids 351 (2005) 1232.
[14] L.Y. Chen, Z.D. Fu, G.Q. Zhang, X.P. Hao, Q.K. Jiang, X.D. Wang, Q.P. Cao, H. Franz, Y.G. Liu, H.S. Xie, S.L. Zhang, B.Y. Wang, Y.W. Zeng, J.Z. Jiang, Phys. Rev. Lett. 100 (2008) 075501.
[15] L. Liu, C.L. Qiu, M. Sun, Q. Chen, K.C. Chan, K.H. Geoffrey, Pang, Mater. Sci. Eng. A 449–451 (2007) 193.
[16] N. Chen, D.V. Louzguine-Luzgin, G.Q. Xie, T. Wada, A. Inoue, Acta Mater. 57 (2009) 2780.
[17] A.A. Kündig, M. Ohnuma, D.H. Ping, T. Ohkubo, K. Hono, Acta Mater. 52 (2004) 2441.
[18] J.C. Oh, T. Ohkubo, Y.C. Kim, E. Fleury, K. Hono, Scripta Mater. 53 (2005) 165.
[19] J. Pan, L. Liu, K.C. Chan, Scripta Mater. 60 (2009) 822.
[20] K.B. Kim, J. Das, X.D. Wang, X. Zhang, J. Eckert, S. Yi, Phil. Mag. Lett. 86 (2006) 479.
[21] E.S. Park, D.H. Kim, Acta Mater. 54 (2006) 2597.
[22] M.H. Lee, J.Y. Lee, D.H. Bae, W.T. Kim, D.J. Sordelet, D.H. Kim, Intermetallics 12 (2004) 1133.
[23] T.C. Hufnagel, C. Fan, R.T. Ott, J. Li, S. Brennan, Intermetallics 10 (2002) 1163.
[24] T.C. Hufnagel, S. Brennan, Phys. Rev. B 67 (2003) 014203.
[25] K.F. Yao, F. Ruan, Y.Q. Yang, N. Chen, Appl. Phys. Lett. 88 (2006) 122106.